Current Biology *18*, 235–244, February 26, 2008 DOI 10.1016/j.cub.2008.01.042

Article

MinC Spatially Controls Bacterial Cytokinesis by Antagonizing the Scaffolding Function of FtsZ

Alex Dajkovic,[2,3,4,*] Ganhui Lan,[1] Sean X. Sun,[1] Denis Wirtz,[2,*] and Joe Lutkenhaus[3]
[1]Department of Mechanical Engineering
Johns Hopkins University
3400 N. Charles Street
Baltimore, Maryland 21218
[2]Department of Chemical Engineering
Johns Hopkins University
3400 N. Charles Street
Baltimore, Maryland 21218
[3]Department of Microbiology, Molecular Genetics, and Immunology
University of Kansas Medical Center
Kansas City, Kansas 66160

Summary

Background: Cytokinesis in bacteria is mediated by a cytokinetic ring, termed the Z ring, which forms a scaffold for recruitment of other cell-division proteins. The Z ring is composed of FtsZ filaments, but their organization in the Z ring is poorly understood. In *Escherichia coli*, the Min system contributes to the spatial regulation of cytokinesis by preventing the assembly of the Z ring away from midcell. The effector of the Min system, MinC, inhibits Z ring assembly by a mechanism that is not clear.
Results: Here, we report that MinC controls the scaffolding function of FtsZ by antagonizing the mechanical integrity of FtsZ structures. Specifically, MinC antagonizes the ability of FtsZ filaments to be in a solid-like gel state. MinC is a modular protein whose two domains ($MinC_C$ and $MinC_N$) synergize to inhibit FtsZ function. $MinC_C$ interacts directly with FtsZ polymers to target MinC to Z rings. $MinC_C$ also prevents lateral interactions between FtsZ filaments, an activity that seems to be unique among cytoskeletal proteins. Because $MinC_C$ is inhibitory in vivo, it suggests that lateral interactions between FtsZ filaments are important for the structural integrity of the Z ring. $MinC_N$ contributes to MinC activity by weakening the longitudinal bonds between FtsZ molecules in a filament leading to a loss of polymer rigidity and consequent polymer shortening. On the basis of our results, we develop the first computational model of the Z ring and study the effects of MinC.
Conclusions: Control over the scaffolding activity of FtsZ probably represents a universal regulatory mechanism of bacterial cytokinesis.

Introduction

The main component of the cytokinetic apparatus in bacteria—the Z ring—is spatially regulated such that its assembly occurs exclusively at midcell [1, 2]. The Z ring consists of FtsZ polymers attached to the membrane through membrane-associated proteins ZipA and FtsA [1]. The remaining proteins required for cytokinesis are recruited to the Z ring to form a complete cytokinetic apparatus, the septal ring, capable of carrying out cytokinesis. Their presence at the division site depends on the integrity of the Z ring [3]. FtsZ polymers are believed to provide mechanical coherence to the Z ring by functioning as a scaffold that organizes and maintains all cell-division proteins. This scaffolding function of FtsZ in cell division is reinforced by recent studies, which found that FtsZ proteins from phylogenetically diverse bacteria can function in *E. coli* provided they are tethered to the membrane through interaction with FtsA and ZipA [4]. How FtsZ filaments cohere to carry out this function is unclear.

The FtsZ molecule appears to have at least four reactive sites through which it can bind to other FtsZ molecules, i.e., FtsZ, appears to be polyvalent. Two sites, one at each end of the monomer, are involved in GTP-dependent longitudinal interactions that lead to the formation of enzymatically active linear filaments that hydrolyze GTP [5]. Two additional sites are involved in lateral interactions between subunits in separate filaments. These interactions lead to the formation of filament bundles and an interconnected polymer network. FtsZ structures composed of such a network feature an elastic modulus; i.e., these FtsZ structures are in a gel state and are measurably stiff and solid like [6]. Lateral interactions between FtsZ filaments are widely hypothesized to be important for the structure of the Z ring [1, 4, 7], but no evidence exists in support of this hypothesis. The polyvalence of FtsZ seems to be a universally conserved character because bundles are observed in assembly reactions of FtsZ molecules from phylogenetically divergent species (see electron micrographs in [8–10]).

The Min system spatially regulates cytokinesis by inhibiting Z ring assembly near the cell poles. The effector of this system is MinC, which is recruited to the membrane by MinD and induced to oscillate by MinE [11–16]. Through this oscillation, the time-averaged concentration of MinC is highest at the poles and lowest at midcell.

The molecular mechanism by which MinC antagonizes Z rings is unknown. A MalE-MinC fusion inhibits FtsZ assembly, as assayed by sedimentation, but has no effect on the GTPase activity of FtsZ [17]. Because the GTPase activity is linked to FtsZ assembly [18, 19], MinC must act after assembly and thereby possibly destabilize FtsZ polymers [17, 20].

MinC is a modular molecule with two structurally and functionally distinct domains: an N-terminal domain ($MinC_N$) and a C-terminal domain ($MinC_C$) [21, 22]. MalE-$MinC_N$, like the full-length MinC, prevents sedimentation of FtsZ [21]. In contrast, MalE-$MinC_C$ has no effect on sedimentation, although it has inhibitory activity in vivo [21, 23]. MinC is a potent inhibitor of Z rings in vivo because of its efficient targeting to the membrane and subsequently to the cytokinetic ring [24, 25]. This targeting to the cytokinetic ring requires $MinC_C$ and MinD; however, the binding partner of the MinD-$MinC_C$ complex in the cytokinetic ring is unknown.

The present model for the mechanism of Min inhibition suggests that the $MinC_C$-MinD complex is targeted to the cytokinetic ring, bringing $MinC_N$ in close proximity to the Z ring [26].

*Correspondence: alex.dajkovic@curie.fr (A.D.), wirtz@jhu.edu (D.W.)
[4]Present address: Institut Curie, UMR 144, 12 rue Lhomond, 75005 Paris, France.

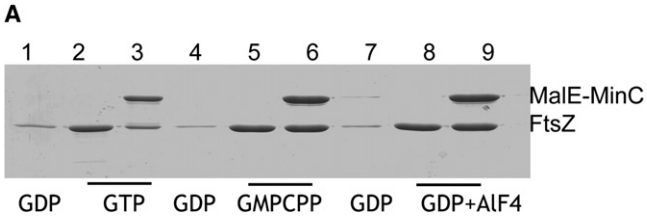

Figure 1. FtsZ GTPase Is Required for MinC's Inhibitory Effect

(A) Effect of nucleotide and MalE-MinC on sedimentation of FtsZ. FtsZ (5 μM) was incubated with GTP (lanes 2 and 3), GMPCPP (lanes 5 and 6), or GDP and AlF_4 (lanes 8 and 9). Controls with GDP are in lanes 1, 4, and 7. An equimolar amount of MalE-MinC was added in lanes 3, 6, and 9.

(B) The products of the polymerization reaction containing FtsZ (5 μM), MalE-MinC (5 μM) and GMPCPP was analyzed by electron microscopy. The scale bar represents 50 nm.

Results

GTPase Activity of FtsZ Is Necessary for Sensitivity to MinC

To examine the role of the GTPase activity of FtsZ in the regulation by MinC, we compared the effect of MalE-MinC on the sedimentation of FtsZ polymers formed in the presence and absence of GTP hydrolysis. FtsZ was polymerized with GTP, GMPCPP, a nonhydrolysable analog of GTP, or with GDP and AlF_4, a mixture that structurally mimics GTP and promotes polymerization. As shown previously, a 1:1 molar ratio of MalE-MinC prevented the pelleting of FtsZ assembled in the presence of GTP (Figure 1A, lanes 1–3). In contrast, MalE-MinC did not prevent the sedimentation of FtsZ assembled in the presence of GMPCPP or GDP and AlF_4 (Figure 1A, lanes 6 and 9, respectively). Electron microscopy confirmed that the products of the reactions with GMPCPP and GDP and AlF_4 were FtsZ polymers (Figure 1B, the results with GMPCPP are depicted; similar results were obtained with GDP and AlF_4). These results argue that the GTPase activity of FtsZ is required for the inhibitory activity of MalE-MinC and imply that dynamic polymers are required for MinC to exert its effect.

MalE-MinC appeared in the pellet in reactions containing GMPCPP or GDP and AlF_4 to a greater extent than in reactions with GTP. This result indicates MalE-MinC adhered to FtsZ polymers. Thus, the failure of MalE-MinC to inhibit the sedimentation of FtsZ polymers assembled in the presence of nonhydolyzable analogs of GTP is unlikely to be due to a failure of MalE-MinC to interact with the FtsZ polymers.

Direct Binding of MalE-$MinC_C$ to FtsZ Polymers

MalE-$MinC_C$ does have inhibitory activity in vivo in the presence of MinD, but less than the full-length protein (Figure S1 available online). To test for direct interaction between $MinC_C$ and FtsZ, we also performed the above described sedimentation experiments with MalE-$MinC_C$. MalE-$MinC_C$ was also enriched in pellets containing FtsZ polymers (Figure 2A). The effect was specific to $MinC_C$ because MalE was not enriched in pellets containing FtsZ (data not shown, see also [17]).

To confirm that $MinC_C$ interacted with polymerized FtsZ, we complemented the high-speed sedimentation experiments with a low-speed phospholipid sedimentation assay developed previously for assessing MinD binding to membranes [27, 28]. We wished to determine whether MinC and/or $MinC_C$ could recruit FtsZ polymers to vesicles containing bound MinD. MinD binds to giant vesicles in the presence of ATP, and these complexes can be sedimented in a tabletop centrifuge. If MalE-MinC or MalE-$MinC_C$ is added to the reactions, they are recruited to the vesicles by interaction with MinD [27, 29, 30].

When FtsZ was polymerized with GMPCPP and included in reactions with the phospholipid vesicles, MinD and ATP, FtsZ polymers did not sediment (Figure 2B, lanes 1 and 2) with MinD and the vesicles. This result confirmed that the g forces used here were insufficient to sediment FtsZ polymers and that FtsZ polymers did not interact with MinD-phospholipid vesicle complexes. In contrast, FtsZ polymerized with GMPPCP was pelleted if either MalE-$MinC_C$ or MalE-MinC were included in the reaction (Figure 2B, lanes 5–8). FtsZ did not sediment if GDP was added (Figure 2B, lane 3 and 4). Such a result indicates that it was polymerized FtsZ that adhered to the vesicles. The amount of FtsZ that sedimented with full-length MalE-MinC was not significantly different from the amount that sedimented with MalE-$MinC_C$, suggesting that the binding observed with the full-length protein can be accounted for by the affinity of polymerized FtsZ for MalE-$MinC_C$. If we used GTP instead of GMPCPP, we did not observe FtsZ in the pellet, indicating that stabilized polymers were required.

To interrogate the structure of sedimenting complexes, we examined the products of the above reactions by EM. When FtsZ, GMPCPP, MalE-$MinC_C$, MinD, ATP, and phospholipids were present in the reactions, vesicles with tubular protrusions were observed (Figure 2C). Both the bodies of the vesicles and the tubular protrusions were coated with polymers, which extended longitudinally along the surface of the protrusions. The spacing between the filaments on these protrusions was irregular—in contrast to the highly regular spacing of FtsZ filaments in bundles. This suggests that the polymers were not organized on the surface on the vesicle because of bundling but rather became aligned after binding to the vesicles. At higher magnifications, the polymers coating the phospholipid vesicle were seen to run off the vesicle and interconnect with the polymer network on the remaining area of the grid (Figure 2D). If MalE-$MinC_C$ was omitted from the reactions, the observed vesicles did not contain protrusions, and the vesicles were not decorated with polymers (Figure 2E). Note that it was previously shown that MinD alone can tubulate vesicles, but this requires a higher molar ratio of MinD to phospholipid, and the tubulated vesicles have a much different appearance [31]. Also, longitudinal polymers coating the vesicles are not observed when MinD alone is added to phospholipids [31].

The experiments presented here demonstrate that $MinC_C$ interacts directly with FtsZ polymers. This result suggests that FtsZ polymers are the binding partner for $MinC_C$ and MinD in the Z ring and that the targeting of MinC to incipient Z rings is mediated through a direct interaction between MinC and FtsZ.

MinC and $MinC_C$ Cause a Concentration-Dependent Decrease in the Elasticity of FtsZ Gels

Although MalE-MinC prevents the pelleting of FtsZ polymers in the sedimentation assay, it does not inhibit the GTPase activity, suggesting it acts after FtsZ polymerizes. Pelleting efficiency is a function of the mass of macromolecular complexes as well as their mechanical stability, i.e., their ability to resist

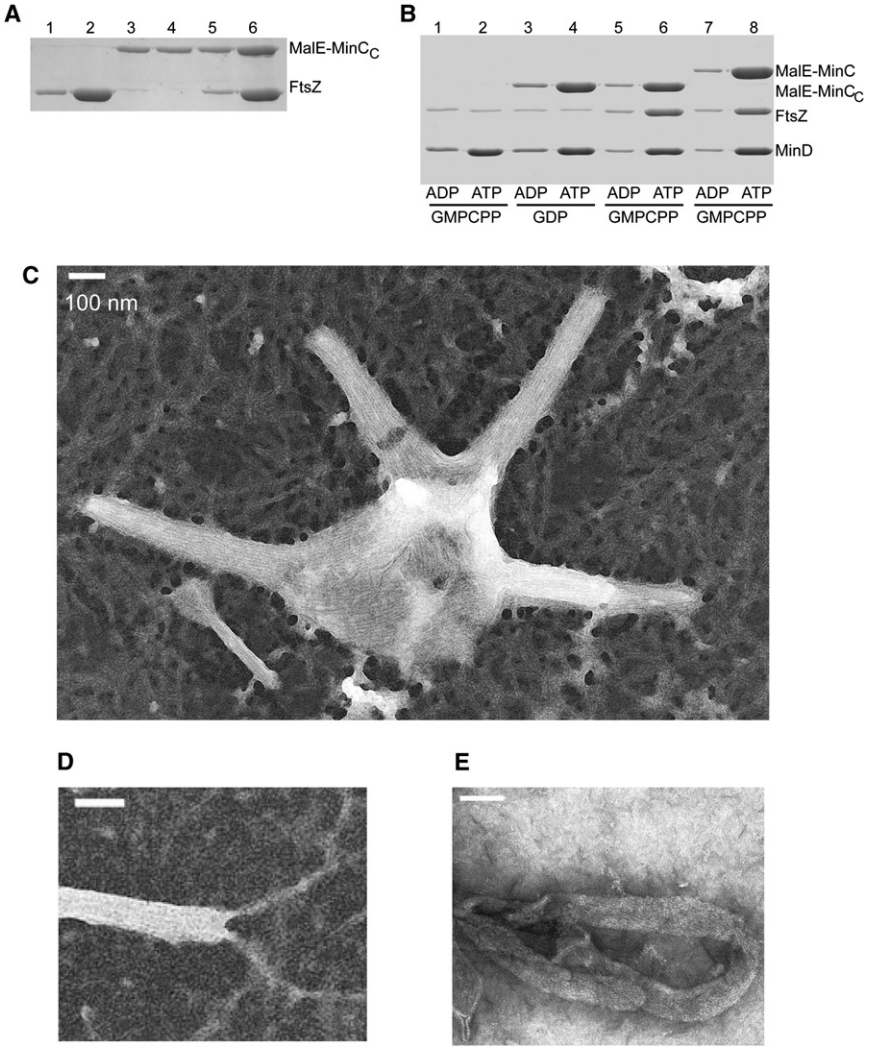

Figure 2. MalE-MinC and MalE-MinC$_C$ Interact with FtsZ Polymers

(A) Reactions were incubated with GDP (lanes 1, 3, and 5) or GMPCPP (lanes 2, 4, and 6). FtsZ (5 μM) was added to reactions in lanes 1, 2, 5, and 6. MalE-MinC$_C$ (5 μM) was added to the reactions in lanes 3–6. After centrifugation, the pellets were analyzed by SDS-PAGE.

(B) Sedimentation assay for the recruitment of FtsZ polymers to MalE-MinC$_C$/MalE-MinC bound to vesicle-associated MinD. MinD (6 μM) and phospholipids (400 μg/mL) were incubated either with ADP (1 mM) or ATP (1 mM). FtsZ was included in the reactions, and either GDP or GMPCPP was added. MalE-MinC was added to lanes 7 and 8. MalE-MinC$_C$ was added to lanes 3–6. The reactions were incubated at room temperature for 5 min and centrifuged at 10,000 g for 2 min. The pellets were solubilized and analyzed by SDS-PAGE.

(C) EM of a reaction containing FtsZ, MalE-MinC$_C$, MinD, vesicles, ATP, and GMPCPP; similar to the conditions in lane 6, (B).

(D) Higher-magnification image from (C), showing FtsZ polymers coating the vesicle and interconnecting with the polymer network on the EM grid.

(E) EM of a control reaction in which MalE-MinC$_C$ was omitted (reaction conditions as in lane 2, [B]).

shear that arises from velocity gradients during centrifugation [32]. It is therefore possible that MinC reduces the size or the mechanical stability of FtsZ polymers. Indeed, in a newly developed FRET assay for polymerization of FtsZ, which does not involve mechanical perturbations [33], MinC does not affect the amount of FtsZ that is in the polymers (see Supplemental Results and Figure S2).

One known in vivo function of FtsZ is the structural maintenance of the cytokinetic ring. This scaffolding function requires that 3D structures formed by FtsZ have sufficient stiffness and mechanical stability to maintain the coherence of the cytokinetic apparatus from the time of the formation of the Z ring through cell separation. Because MinC did not block FtsZ polymerization, it may antagonize this scaffolding function of FtsZ.

To quantify the stiffness of FtsZ networks and to assess the effects of MinC, we used quantitative rheometry to measure the elastic modulus of FtsZ networks (see Experimental Procedures). The elastic modulus quantifies the propensity of polymer networks to rebound after deformations, i.e., it measures their stiffness.

Addition of GTP to solutions of FtsZ (1 mg/ml) led to a rapid onset of elasticity (Figure 3A), reaching a plateau in 3–5 min, as described previously [6]. Various amounts of MalE-MinC were added to FtsZ networks that had attained a steady-state level of elasticity, and the elastic modulus was measured as a function of time. Addition of MalE-MinC led to a decrease in elasticity, i.e., FtsZ networks became less stiff (Figure 3A). This decrease in stiffness of FtsZ networks depended on the concentration of MalE-MinC (Figure 3B). When MalE-MinC was present in 2-fold excess over FtsZ, the elastic modulus decreased rapidly and became vanishingly low (Figures 3A and 3B), reaching values obtained for buffer alone. This result indicates that an excess of MinC completely eliminated the stiffness of the FtsZ network, i.e., MalE-MinC liquefied FtsZ structures. This effect on elasticity was specific to MinC because MalE had no detectable effect when added to the reactions (Figure 3F).

Because MalE-MinC prevents the sedimentation of FtsZ without inhibiting polymerization, we hypothesized that mechanical perturbations, such as shear forces generated during centrifugation [32], could enhance the inhibitory effects of MinC. To test this hypothesis, we assembled FtsZ networks by addition of GTP. After steady-state elasticity was reached, we added MalE-MinC. The networks were then immediately subjected to a cycle of large shear deformations (see Experimental Procedures), and the elasticity was measured as a function of time. A pure FtsZ network lost all of its stiffness after large deformations, but it recovered very rapidly (Figure 3C). When MalE-MinC was present, large shear deformations caused a loss of stiffness that did not recover on the time scale of the experiment (Figure 3C). This result suggests that mechanical perturbations can greatly enhance the inhibitory effects of MalE-MinC.

Next, we tested the effects of MalE-MinC$_C$ on the elasticity of FtsZ structures. MalE-MinC$_C$ also led to a concentration-dependent decrease in the stiffness of FtsZ networks (Figures 3D and 3E), but the effect was somewhat smaller than with

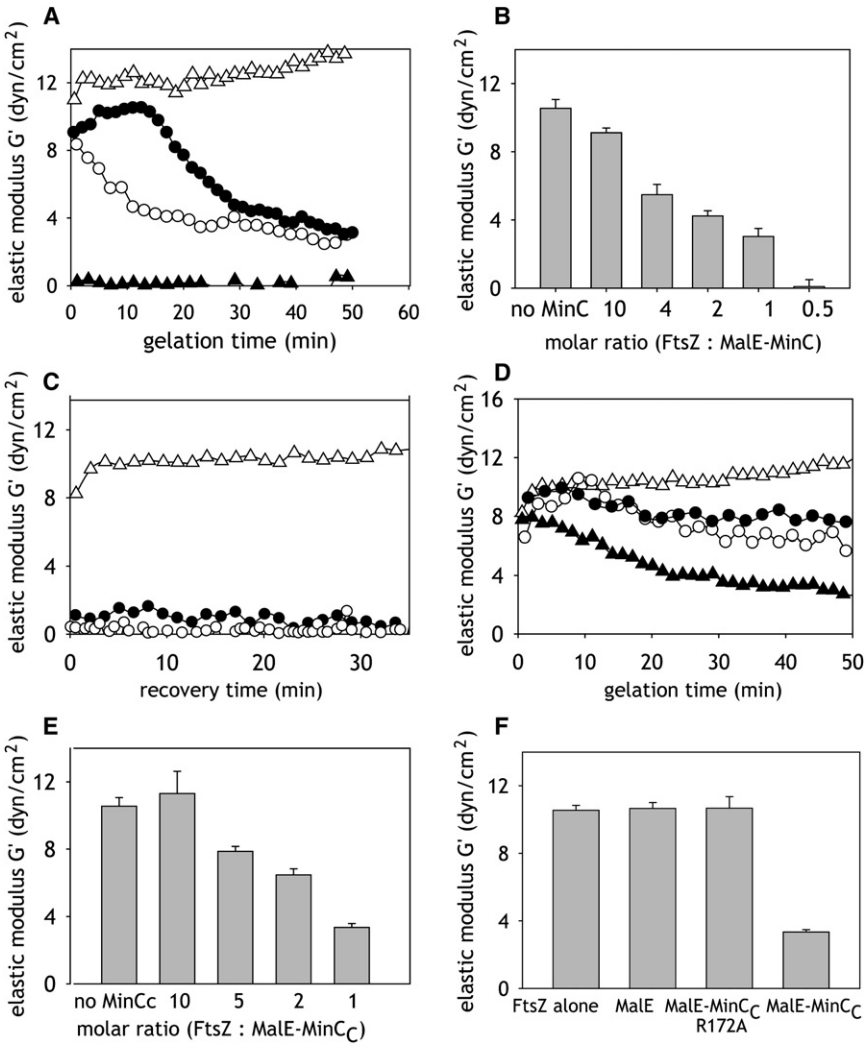

Figure 3. MinC Antagonizes the Mechanical Integrity of FtsZ Structures

(A) The effect of MalE-MinC on FtsZ polymer networks that had attained a steady-state level of elasticity. FtsZ alone (triangles), FtsZ:MalE-MinC molar ratio 2:1 (filled circles), FtsZ:MalE-MinC molar ratio 1:1 (open circles), FtsZ:MalE-MinC molar ratio 1:2 (filled triangles) are shown.

(B) Dependence of the steady-state value of elasticity for FtsZ polymer networks on the concentration of MalE-MinC (at the indicated molar ratios of FtsZ to MalE-MinC).

(C) Effects of large shear deformations and MalE-MinC on the stiffness of FtsZ networks. FtsZ networks were allowed to attain a steady-state level of elasticity, and MalE-MinC was added at molar ratios of 2:1 (filled circles) and 1:1 (empty circles). The networks were then subjected to large shear deformation, and the recovery of elasticity was monitored as a function of time. Pure FtsZ networks (triangles) recover their elasticity very rapidly, whereas networks formed in the presence of MalE-MinC (circles) did not recover.

(D) The effect of MalE-$MinC_C$ on the elasticity of FtsZ networks. The gelation kinetics of FtsZ networks was followed after MalE-$MinC_C$ was added to FtsZ networks that had attained a steady-state level of elasticity. FtsZ alone (triangles), FtsZ:MalE-$MinC_C$ molar ratio 2:1 (filled circles), FtsZ:MalE- $MinC_C$ molar ratio 1:1 (empty circles), FtsZ:MalE-MinC molar ratio 1:2 (filled triangles) are shown.

(E) Concentration dependence of the steady-state value of elasticity for FtsZ polymer networks in the presence MalE-$MinC_C$ at the indicated molar ratios (FtsZ to MalE-MinC).

(F) Specificity of the effects of MalE-MinC and MalE-$MinC_C$ on the elasticity of FtsZ polymer networks. The effects of MalE, MalE-$MinC_C$-R172A, and MalE-MinC on the elasticity of FtsZ (molar ratios 1:1). In all panels, error bars denote 95% confidence intervals.

MalE-MinC. To test the specificity of these effects, we used the MalE-$MinC_C$-R172A mutant protein, which abolishes the targeting of $MinC_C$ to the Z ring and impairs its ability to inhibit Z ring formation [23, 29]. MalE-$MinC_C$-R172A had no detectable effect on the elasticity of FtsZ networks, further indicating that the effects observed by rheometry were specific (Figure 3F).

The rheometry studies show that both MinC and $MinC_C$ diminish the stiffness of FtsZ structures. Furthermore, mechanical perturbations greatly accelerate the inhibitory effects of MalE-MinC.

Ultrastructure of FtsZ Polymer Networks in the Presence of MinC and $MinC_C$

Our results indicated that MinC did not affect the amount of polymerized FtsZ, although it did affect the elasticity of the network formed by FtsZ. To establish the structural basis for the effects of MalE-MinC and MalE-$MinC_C$ on FtsZ, we used EM. Under standard buffer conditions, FtsZ formed interconnected polymer networks (Figure 4A). These networks consisted of filaments, bundles of filaments, and branching bundles (Figure 4A, inset) with interconnections between polymer species. The spacing of filaments in bundles was highly regular.

Addition of equimolar amounts of MalE-$MinC_C$ to the polymerization reactions led to a dramatic alteration of the polymer network. There was a decrease in the number of interpolymer contacts (Figure 4B). The polymers were long and had multiple points of entanglement (Figure 4B, inset), but lateral interactions between polymers were predominantly absent. To quantify the presence of bundles in a network, we measured the thickness of polymer species found in random sectors of electron micrographs containing pure FtsZ networks and FtsZ networks formed in the presence of equimolar amounts of MalE-$MinC_C$. Pure FtsZ networks were composed of polymer species with a wide distribution of widths that result from the presence of bundles containing various numbers of filaments (Figure 4D). On the other hand, polymer species formed with equimolar amounts of MalE-$MinC_C$ had a narrow distribution of widths (Figure 4D), indicating that $MinC_C$ antagonized the bundling of FtsZ filaments. The mean width of polymer species present in pure FtsZ networks was significantly greater ($p < 0.00001$) than the mean width of FtsZ networks formed with equimolar amounts of MalE-$MinC_C$ (Figure 4G). The mean width of polymer species formed in the presence of MalE-$MinC_C$ is consistent with a pair of filaments or with a filament coated with MalE-$MinC_C$.

We next tested the effects of full-length MalE-MinC on FtsZ polymer networks. We wanted to determine what effect full-length MinC had that was responsible for inhibiting FtsZ sedimentation. Any activity in addition to the debundling activity associated with $MinC_C$ would be attributable to $MinC_N$. As

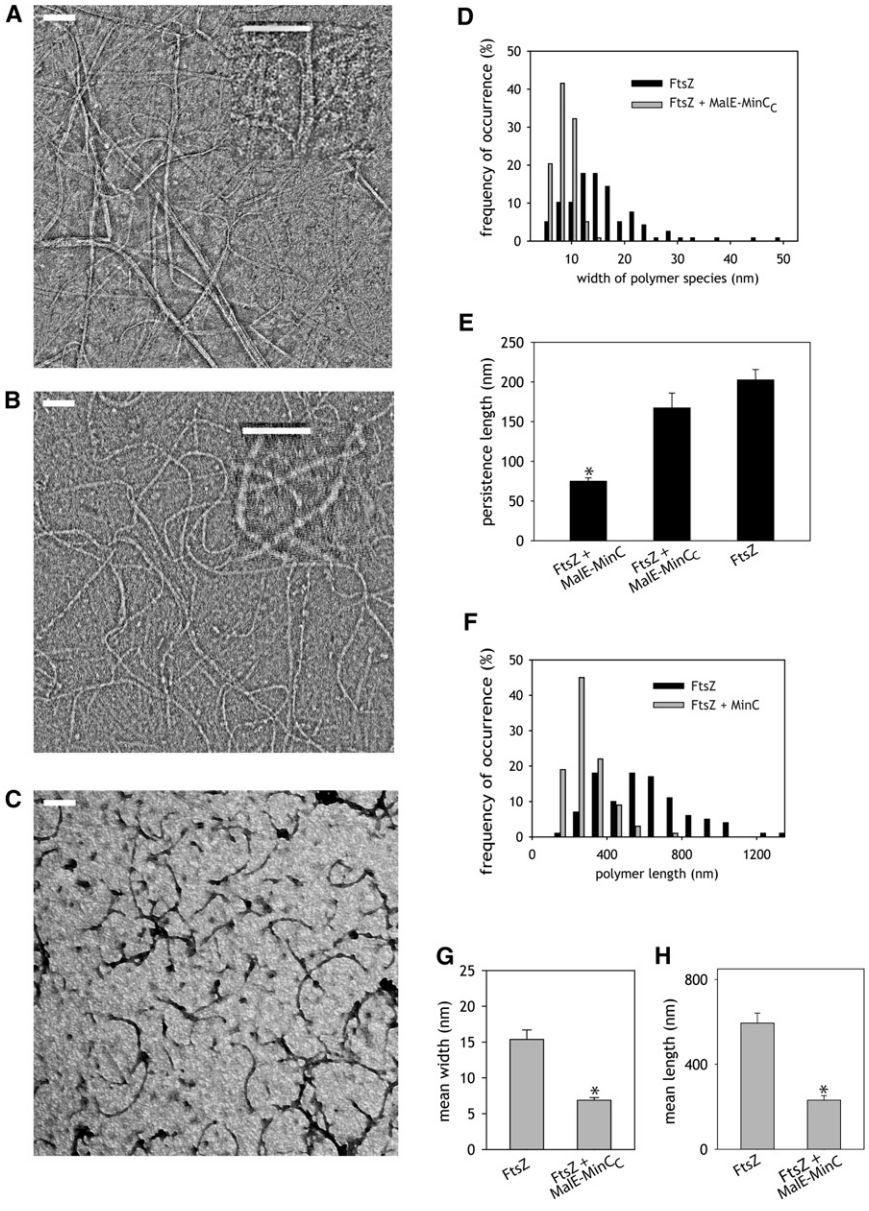

Figure 4. Effect of MalE-MinC and MalE-MinC$_C$ on FtsZ Polymer Networks as Determined by Electron Microscopy

(A) FtsZ (5 μM) forms a polymer network that displays bundling. The inset shows the detail of a polymers branching off a bundled structure.

(B) FtsZ (5 μM) polymer network formed in the presence of equimolar amounts of MalE-MinC$_C$ shows entanglements, but there is a loss of bundling and lateral interconnections between polymers. The inset shows the detail of entanglements between polymers.

(C) FtsZ (5 μM) polymers formed in the presence of equimolar amounts of MalE-MinC.

(D) Distribution of thickness of polymer species present in pure FtsZ (5 μM) networks and FtsZ networks formed with equimolar amounts of MalE-MinC$_C$.

(E) Mean persistence length of FtsZ polymer species in the absence of any additions and in the presence of MalE-MinC or MalE-MinC$_C$.

(F) Length distribution of FtsZ polymers formed in the absence or presence of equimolar amounts of MalE-MinC.

(G) Mean thickness of FtsZ polymers formed in the absence or presence of equimolar amounts of MalE-MinC$_C$.

(H) Mean length of FtsZ polymers formed with or without equimolar amounts of MalE-MinC. In all panels, error bars denote 95% confidence intervals, and asterisks indicate a highly significant difference ($p < 0.00001$). The scale bars represent 100 nm throughout.

expected, FtsZ polymers formed in the presence of equimolar amounts of MalE-MinC showed a decreased width and a loss of interfilament contacts (Figure 4C). In addition, these polymers were shorter and had an increasingly curved appearance. We analyzed images of FtsZ polymers formed in the presence of MalE-MinC to assess their persistence length. The persistence length is the length scale over which a polymer maintains its straight shape; it is proportional to polymer rigidity. FtsZ polymers formed in the presence of equimolar amounts of MalE-MinC showed significant differences ($p < 0.00001$) in persistence lengths in comparison to pure FtsZ. Although pure FtsZ polymers had a mean persistence length of 180 nm, FtsZ polymer species formed in the presence of equimolar amounts of MalE-MinC had a mean persistence length of 80 nm (Figure 4E). FtsZ polymer species formed in the presence of equimolar amount of MalE-MinC$_C$ had a mean persistence length of 160 nm (Figure 4E).

The observed decrease in the persistence length of FtsZ polymers formed in the presence of MalE-MinC indicates that MalE-MinC decreases the rigidity of the filaments. This suggests that MinC strains the longitudinal bond formed between FtsZ subunits. To assess whether this effect leads to filament fragility and breakage, we analyzed polymer-length distribution of FtsZ polymers formed in the presence and absence of equimolar amounts of MalE-MinC (Figure 4F). FtsZ polymers formed in the presence of MalE-MinC were significantly shorter ($p < 0.00001$) than pure FtsZ polymers (Figure 4H). The mean polymer length was 2-fold lower (Figure 4H). Note that even in the presence of MalE-MinC, polymers are sufficiently long that they would be expected to be sedimented by centrifugation. The fact that the polymers are not sedimented at these concentrations of FtsZ and MalE-MinC is consistent with MinC rendering FtsZ polymers more fragile and susceptible to breakage because of mechanical stresses that arise during centrifugation.

The above ultrastructural studies suggest the basis for the inhibitory activities of MinC$_C$ and MinC. MalE-MinC$_C$ does not depolymerize FtsZ polymers but rather debundles them, an activity not displayed by any microtubule or actin-binding proteins. In addition, full-length MinC, because of the presence of MinC$_N$, decreases the rigidity of FtsZ polymers and makes them easier to break under mechanical stress.

ZapA Reverses the Inhibitory Effects of MinC and MinC$_C$

If the activity of MinC, in part, involves the reduction of lateral interactions between FtsZ filaments, then factors that promote

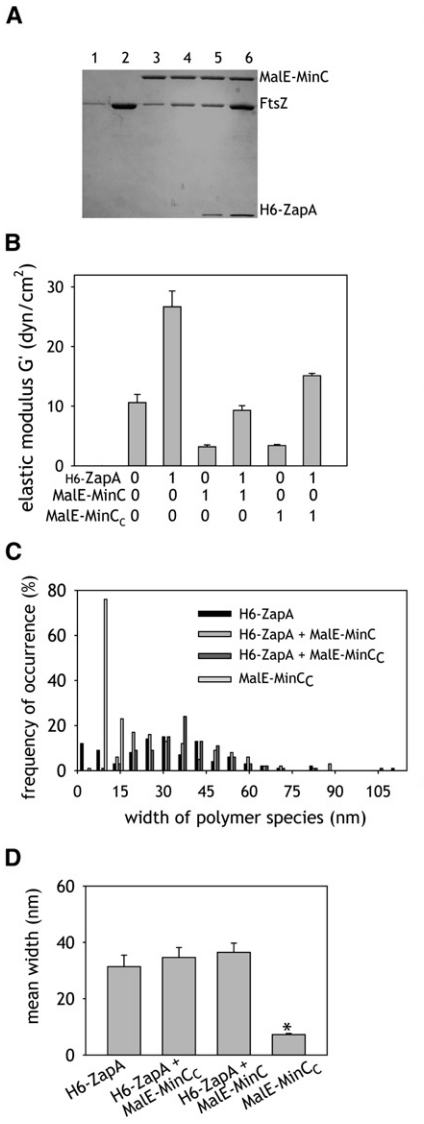

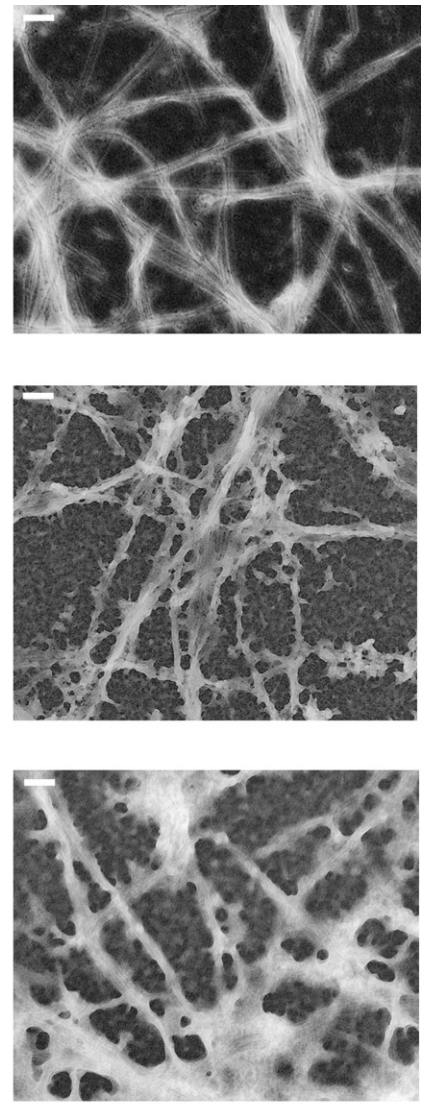

Figure 5. The Effects of H6-ZapA on the Inhibition of FtsZ by MalE-MinC and MalE-MinC$_C$

(A) H6-ZapA restores pelleting of FtsZ in the presence of MalE-MinC. FtsZ (5 μM) was polymerized with GTP (lane 2), in the presence of 5 μM MalE-MinC (lane 4), or in the presence of 5 μM MalE-MinC and 5 μM H6-ZapA (lane 6). Lanes 1, 3, and 5 are controls with GDP.

(B) The effect of H6-ZapA on the elasticity of FtsZ networks in the presence of MalE-MinC and MalE-MinC$_C$. Molar ratios to FtsZ are indicated below the bar graph.

(C) Distribution of thickness of polymer species formed in the presence of MalE-MinC$_C$, MalE-MinC + H6-ZapA, MalE-MinC$_C$ + H6-ZapA, and H6-ZapA.

(D) Mean thickness of polymer species.

(E) EM of FtsZ polymer networks (5 μM) formed in the presence of equimolar amounts of H6-ZapA.

(F) EM of FtsZ polymer networks (5 μM) formed in the presence of equimolar amounts of H6-ZapA and MalE-MinC.

(G) FtsZ polymer networks (5 μM) formed in the presence of equimolar amounts of H6-ZapA and MalE-MinC$_C$. Scale bars represent 100 nm throughout. In all panels, error bars denote 95% confidence intervals, and asterisks indicate significant difference ($p < 0.00001$).

FtsZ-filament bundling might be expected to antagonize this activity. One protein known to promote the bundling of FtsZ filaments is ZapA [7]. We first used the sedimentation assay to study the effect of ZapA on the assembly of FtsZ in the presence of MalE-MinC. Addition of equimolar amounts of hexahistidine-tagged ZapA (H6-ZapA) to polymerization reactions containing FtsZ and MalE-MinC (in a 1:1 molar ratio) restored the sedimentation of FtsZ (Figure 5A). This restoration of FtsZ sedimentation by H6-ZapA also resulted in a reduction in the amount of MalE-MinC in the pellet, suggesting ZapA and MinC might compete for binding to FtsZ.

Next, we tested whether H6-ZapA could reverse the softening of FtsZ structures observed in the presence of equimolar amounts of MalE-MinC or MalE-MinC$_C$. Inclusion of equimolar amounts of H6-ZapA in the polymerization reactions with MalE-MinC or MalE-MinC$_C$ restored the elasticity of FtsZ networks (Figure 5B). Interestingly, the steady-state elastic modulus of FtsZ networks polymerized in the presence of equimolar amounts of H6-ZapA and MalE-MinC or MalE-MinC$_C$ had approximately the same magnitude as the elastic modulus of pure FtsZ networks, whereas the elastic modulus of FtsZ/H6-ZapA networks had a much higher magnitude (Figure 5B). This indicates that ZapA and MinC have opposing activities on the stiffness of FtsZ structures.

We complemented the centrifugation and rheometry studies with EM (Figures 5E–5G). FtsZ polymer networks formed in the presence of equimolar amounts of H6-ZapA showed extensive bundling, and single filaments were seldom detected (Figure 5E). FtsZ networks produced in the presence of equimolar amounts of MalE-MinC and H6-ZapA had an indistinguishable network structure (Figure 5F). The polymers were long, and significant interfilament interactions were readily observed. Addition of equimolar amounts of H6-ZapA to FtsZ-filament networks formed in the presence of equimolar amounts of MalE-MinC$_C$ likewise led to a reconstitution of interfilament interactions, and bundles of polymers were readily observed (Figure 5G). Quantification of polymer widths showed that FtsZ polymer species formed in the presence of H6-ZapA alone, with H6-ZapA and MalE-MinC, or ZapA and MalE- MinC$_C$, did not vary significantly in mean thickness (Figures 5C and 5D).

These results suggest that MinC and ZapA have antagonistic activities on the scaffolding activity of FtsZ.

A Model of the Z Ring and the Activity of MinC

To test the idea that the interactions outlined above are sufficient to account for the observed behavior, we constructed a computational model for FtsZ structures and examined the effects of MinC. We asked: (1) What structures emerge spontaneously from the simple network of longitudinal and lateral interactions between FtsZ molecules outlined above? (2) In what regions of parameter space do these structures correspond to the structures observed experimentally? (3) What is the effect of MinC on these structures?

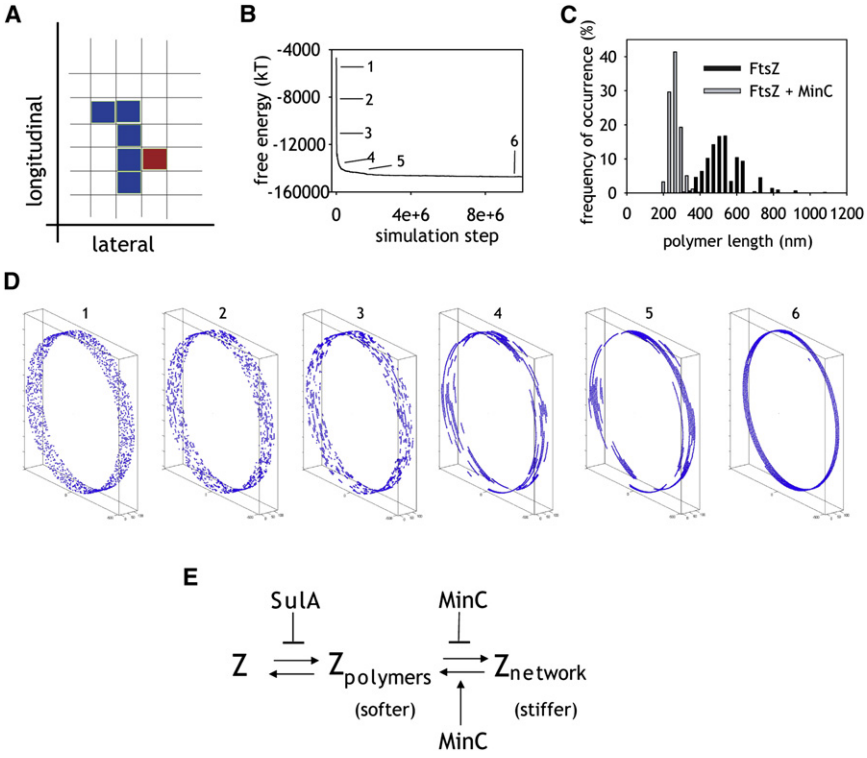

Figure 6. Computational Model of FtsZ-FtsZ and FtsZ-MinC Interactions

(A) Schematic representation of the lattice used in simulations. Blue squares represent FtsZ; red squares represent MinC.

(B) Evolution of the energy of the system when FtsZ interactions are simulated on a cylindrical geometry commensurate with the size of the Z ring with interaction energies outlined in Table 1. Numbers indicate points at which images of rings were extracted for (D).

(C) Effects of MinC on the polymer-length distribution of FtsZ when the energy of longitudinal interaction between FtsZ molecules is decreased 35%.

(D) Evolution of the distribution of FtsZ molecules on the cylindrical lattice. Spatially random distribution of FtsZ molecules (1) represents a high-energy state. As the energy decreases, the system passes through states of increasing connectivity (2–5) until it reaches equilibrium as a contiguous ring (6).

(E) Diagrammatic representation of the equilibria of FtsZ and the effects of MinC, contrasted with SulA.

Because FtsZ self-assembly in the cell and the activity of MinC occur on the 2D surface of the cytoplasmic membrane, we used an Ising-like 2D lattice model. Each lattice box was defined to be 5 nm in size. It could be occupied by an FtsZ molecule or a MinC molecule, or it could be empty (Figure 6A). FtsZ molecules were treated as having the potential to interact with one another longitudinally, with energy $\varepsilon_{Z|Z}$, and laterally, with energy $\varepsilon_{Z\text{-}Z}$. MinC was allowed to bind to FtsZ molecules with the energy $\varepsilon_{Z\text{-}C}$. When MinC was bound to an FtsZ molecule, this FtsZ molecule was prevented from interacting with other FtsZ molecules laterally. Furthermore, when MinC was bound to FtsZ, the energy of longitudinal interaction between FtsZ molecules ($\varepsilon_{Z|Z}$) was decreased to a new value ($\varepsilon_{Z|ZC}$).

We computed the energy evolution of the system by performing equilibrium Monte Carlo simulations with fixed ambient concentrations of FtsZ molecules. We were interested in finding interaction energies $\varepsilon_{Z|Z}$, $\varepsilon_{Z\text{-}Z}$, $\varepsilon_{Z\text{-}C}$, and $\varepsilon_{Z|ZC}$ that would give rise to structures in accordance with what we observed experimentally. First, we scanned parameter space to find the energies for longitudinal and lateral bonds between FtsZ molecules. We found good agreement with experimentally measured polymer lengths only when the longitudinal interactions between FtsZ molecules $\varepsilon_{Z|Z}$ were ~100 times stronger, on a per-molecule basis, than the lateral-interaction energy $\varepsilon_{Z\text{-}Z}$. In particular, we found a good fit with experimental data (Figure S3) when the longitudinal-interaction energy was ~5.4 kcal/mol and the lateral-interaction energy was ~0.06 kcal/mol (Table 1). If the lateral-interaction energy was increased and the longitudinal-interaction energy kept constant, the polymer species were on average significantly shorter and more bundled at equilibrium than what we observed with EM for the same concentrations of FtsZ (data not shown).

Once we obtained reasonable values for the longitudinal- and lateral-interaction energies, we wanted to examine the structures that could emerge spontaneously on a cylindrical geometry commensurate with the size of Z rings in vivo. We wanted to know whether the low-energy structures would be random or whether order would arise spontaneously. On a cylindrical lattice, the energy landscape is characterized by a low-energy state of high connectivity. Starting with a spatially random initial distribution of FtsZ molecules, contiguous rings develop as low-energy configurations of FtsZ molecules (Figures 6B and 6D).

We then proceeded to test the effects of MinC on FtsZ polymer-length distribution. Only when $\varepsilon_{Z|ZC}$ was 60%–65% of $\varepsilon_{Z|Z}$ did the simulation yield a polymer-length distribution that was the same as those measured experimentally for the same concentration of FtsZ (Figure 6C). If the value of $\varepsilon_{Z|ZC}$ was changed significantly outside of this range, the computed polymer-length distribution did not compare favorably with experimentally measured values.

These results demonstrate that a simple network of interactions between FtsZ molecules can capture the behavior of FtsZ. They also show that FtsZ has a tendency to organize into ring structures when polymerized on a cylindrical surface commensurate with the size of the Z ring. Additionally, simple assumptions concerning the activity of MinC supported by our experiments are sufficient to reproduce the effects of MinC.

Table 1. Energies of Interactions Used in the Simulations

$\varepsilon_{Z\|Z}$	$\varepsilon_{Z\text{-}Z}$	$\varepsilon_{Z\|ZC}$	$\varepsilon_{Z\text{-}C}$
−5.4 kcal/mol	−0.06 kcal/mol	−1.8 kcal/mol	−3.6 kcal/mol

Discussion

In this study, we examined the effect of MinC on FtsZ assembly and found that it antagonizes FtsZ assembly at two levels

subsequent to polymerization. It does this through two structurally and functionally distinct domains. $MinC_C$ has affinity for FtsZ filaments and prevents their lateral association. Furthermore, the presence of $MinC_N$ in full-length MinC lowers the rigidity of FtsZ filaments, making them more susceptible to breaking. The combination of these activities leads to a decrease in the stiffness of 3D structures formed by FtsZ and appears necessary for inhibition of Z ring assembly at physiological levels of Min proteins.

An enigma concerning MinC was that it inhibited the sedimentation of FtsZ without inhibiting the GTPase. Our results suggest that the reason for this apparent contradiction lies in the nature of the inhibitory activity of MinC; it reduces the rigidity of FtsZ polymers, making them easier to break. The standard sedimentation assay gives rise to velocity gradients generating shear forces [32] that presumably break FtsZ filaments modified by MinC. This in vitro activity of MinC is due to $MinC_N$, which is also required for MinC to be an effective inhibitor in vivo.

Targeting MinC to the Z Ring

The inhibitory activity of MinC in vivo is enhanced in the presence of coactivators, MinD or DicB, which aid in targeting MinC to the cytokinetic ring [25]. This targeting requires $MinC_C$ and is abolished by the R172A mutation [29]. The MinC-MinD complex is restricted to the poles of the cell through the Min oscillation where it antagonizes nascent Z rings [14, 2]. The component of the Z rings required for targeting of the MinC-MinD complex was not previously identified, although other early recruits to the Z ring (FtsA, ZipA, and ZapA) were ruled out [26]. Our results argue that this component is FtsZ because MalE-$MinC_C$ has affinity for FtsZ polymers and FtsZ polymers are recruited to vesicles coated with MalE-$MinC_C$ and MinD. The targeting of $MinC_C$ in vivo is not observed in the absence of MinD, indicating that MinD enhances this activity by concentrating $MinC_C$ on the membrane and/or further increasing its affinity for FtsZ.

Modeling the Z Ring and MinC

We studied a simple computational model of FtsZ assembly and investigated the effect of MinC. We started with the assumption that an FtsZ molecule can interact with other FtsZ molecules through longitudinal as well as lateral interactions—an assumption supported by the present results. The longitudinal interactions are well established, and support for the importance of lateral interactions is provided in this work. We find that the lateral interactions have to be 100 times weaker, on a per-molecule basis, than the longitudinal interactions to give rise to structures of FtsZ observed in vitro. Even with this weak lateral attraction on a per-molecule basis, significant lateral attraction arises at the level of FtsZ filaments to give rise to bundling, i.e., a polymer 100 subunits long would interact with another polymer of the same length with the same energy as with another monomeric subunit. For longer polymers, lateral interactions become even more favorable.

When the simple network of longitudinal and lateral interactions is implemented on a cylindrical lattice, commensurate with the size of the cell, it generates a ring structure as the lowest energy configuration.

The effects of MinC observed in vitro can be reproduced with assumptions that are supported in this study. The computational results show that a simple network of interactions with defined energies can capture the effect of MinC on FtsZ assembly.

Scaffolding Function of FtsZ and the Importance of Lateral Interactions

The function of the cytokinetic ring depends on its continued persistence as a coherent structure during the entire cytokinetic process. The scaffolding function of the Z ring demands that it possess sufficient mechanical strength to maintain all cell-division proteins at the division site. Our results suggest that spatial control of cell division by MinC is exerted over this character of FtsZ. MinC is a particularly potent inhibitor of FtsZ because it has two inhibitory domains ($MinC_C$ and $MinC_N$) that have synergistic functions. $MinC_C$ binds to FtsZ filaments and prevents them from interacting laterally and forming bundles and stiff networks (Figures 3D and 4B). The debundling activity of $MinC_C$, seemingly unique among eukaryotic and prokaryotic cytoskeletal proteins, causes a decrease in the stiffness of 3D FtsZ structures, such as the Z ring. Importantly, $MinC_N$ has an affinity for FtsZ monomers, and in the context of full-length MinC, it causes FtsZ filaments to break more easily. The loss of interfilament interactions combined with filament shortening antagonize the mechanical integrity of FtsZ structures, which is essential for the scaffolding function of FtsZ in cell division.

Interestingly, the GTPase activity is required for the inhibition of FtsZ assembly by MinC. This further reinforces the necessity of the debundling activity of $MinC_C$, because FtsZ in bundles has reduced GTPase activity as a result of a conformational change in the GTP moiety induced by lateral interactions between FtsZ filaments [34, 35]. Therefore, maximum MinC activity involves inhibition of lateral interactions between FtsZ filaments by $MinC_C$, so they can hydrolyze GTP and thereby become sensitive to the activity of $MinC_N$. This debundling function of $MinC_C$ exists in addition to its targeting function.

It is interesting to note the difference between prokaryotic FtsZ and eukaryotic actin and tubulin. Actin and tubulin form polymers (actin microfilaments and microtubles) that do not have significant self-interactions without accessory proteins. In contrast, FtsZ forms polymers that have significant interactions with one another without accessory proteins. However, both in prokaryotes and in eurkaryotes, interactions between cytoskeletal polymers are regulated by the cell. Lateral interactions between FtsZ filaments are significant not only because of their uniqueness among cytoskeletal proteins but also because their stabilization may represent one possible evolutionary trajectory from FtsZ to tubulin.

Our results suggest that lateral interactions between FtsZ filaments have a clear functional importance. In particular, the fact that $MinC_C$ inhibits lateral interactions in vitro and has inhibitory activity toward Z rings in vivo ([23], see also Supplemental Results), argues that lateral contacts between FtsZ filaments are important for the assembly of the Z ring and for its structural integrity. This is particularly significant because the considerable turnover of FtsZ subunits in the ring [36] poses a question regarding the nature of the coherence of the Z ring as a structure that persists through space and time. If we consider the fact that FtsZ filaments in the Z ring interact with one another at multiple points through lateral contacts, then the turnover of FtsZ subunits in the Z ring will not affect the integrity of the ring. This will be true provided that the number of lateral contacts is above a certain critical value and that there are multiple sites where subunits can be removed from the ring and added back. It will be interesting to determine the exact number of contacts that is necessary to maintain the integrity of the Z ring and the number of sites through which turnover can occur.

ZapA was isolated as a suppressor of elevated MinCD activity and is known to bundle FtsZ filaments [7]. Here, we found that ZapA suppressed the inhibitory activities of MinC in vitro, indicating that it could overcome both the debundling activity of the $MinC_C$ domain and the destabilizing effects of the $MinC_N$ domain. The structural basis of the latter activity of ZapA is not clear because ZapA has been shown so far to only promote lateral interactions between FtsZ filaments [7].

In the aquatic bacterium *Caulobacter crescentus*, no Min system exists. Spatial regulation of the Z ring is effected through an unrelated protein termed MipZ [8]. MipZ seems to control the assembly of FtsZ in a mechanism similar to MinC. Examination of electron micrographs of *Caulobacter crescentus* FtsZ in the presence of MipZ reveals that FtsZ filaments have lost their lateral contacts and that they appear less rigid, i.e., more curved [8]. On the basis of these similarities, it is tempting to speculate that control of the rigidity of FtsZ filaments, as well as the control over the extent of lateral contacts between FtsZ filaments, represents a universally conserved mechanism for regulating cytokinesis in bacteria.

Supplemental Data

Additional Results, Experimental Procedures, and three figures are available at http://www.current-biology.com/cgi/content/full/18/4/235/DC1/.

Acknowledgments

The authors would like to acknowledge Enrique de la Cruz for discussions and critiques and Harold Erickson for the gift of the FtsZ-F268C plasmid. Acknowledgment and gratitude are also due to Barbara Fegley and Karen Grantham of the KUMC Electron Microscopy Research Lab for their enthusiasm and generosity in imaging FtsZ filaments under various conditions. Thanks also go to Marc Ostermeier and the members of his lab and Alexey Ladokhin and members of his lab for the use of their fluorimeters. Ned Perkins and Michael McCaffery from the Integrated Imaging Center at Johns Hopkins University are acknowledged for their help with imaging. This work was supported by NIH GM29764 to J.L. and NIH GM075305 to S.X.S. and D.W.

Received: October 25, 2007
Revised: December 21, 2007
Accepted: January 4, 2008
Published online: February 21, 2008

References

1. Dajkovic, A., and Lutkenhaus, J. (2006). Z ring as executor of bacterial cell division. J. Mol. Microbiol. Biotechnol. *11*, 140–151.
2. Lutkenhaus, J. (2007). Assembly dynamics of the bacterial MinCDE system and spatial regulation of the Z ring. Annu. Rev. Biochem. *76*, 539–562.
3. Addinall, S.G., Cao, C., and Lutkenhaus, J. (1997). Temperature shift experiments with an ftsZ84(Ts) strain reveal rapid dynamics of FtsZ localization and indicate that the Z ring is required throughout septation and cannot reoccupy division sites once constriction has initiated. J. Bacteriol. *179*, 4277–4284.
4. Osawa, M., and Erickson, H.P. (2006). FtsZ from divergent foreign bacteria can function for cell division in Escherichia coli. J. Bacteriol. *188*, 7132–7140.
5. Nogales, E., and Wang, H.W. (2006). Structural mechanisms underlying nucleotide-dependent self-assembly of tubulin and its relatives. Curr. Opin. Struct. Biol. *16*, 221–229.
6. Esue, O., Tseng, Y., and Wirtz, D. (2005). The rapid onset of elasticity during the assembly of the bacterial cell-division protein FtsZ. Biochem. Biophys. Res. Commun. *333*, 508–516.
7. Gueiros-Filho, F.J., and Losick, R. (2002). A widely conserved bacterial cell division protein that promotes assembly of the tubulin-like protein FtsZ. Genes Dev. *16*, 2544–2556.
8. Thanbichler, M., and Shapiro, L. (2006). MipZ, a spatial regulator coordinating chromosome segregation with cell division in Caulobacter. Cell *126*, 147–162.
9. Low, H.H., Moncrieffe, M.C., and Lowe, J. (2004). The crystal structure of ZapA and its modulation of FtsZ polymerisation. J. Mol. Biol. *341*, 839–852.
10. Haeusser, D.P., Schwartz, R.L., Smith, A.M., Oates, M.E., and Levin, P.A. (2004). EzrA prevents aberrant cell division by modulating assembly of the cytoskeletal protein FtsZ. Mol. Microbiol. *52*, 801–814.
11. Hale, C.A., Meinhardt, H., and de Boer, P.A. (2001). Dynamic localization cycle of the cell division regulator MinE in Escherichia coli. EMBO J. *20*, 1563–1572.
12. Hu, Z., and Lutkenhaus, J. (1999). Topological regulation of cell division in Escherichia coli involves rapid pole to pole oscillation of the division inhibitor MinC under the control of MinD and MinE. Mol. Microbiol. *34*, 82–90.
13. Raskin, D.M., and de Boer, P.A. (1999). MinDE-dependent pole-to-pole oscillation of division inhibitor MinC in Escherichia coli. J. Bacteriol. *181*, 6419–6424.
14. Raskin, D.M., and de Boer, P.A. (1999). Rapid pole-to-pole oscillation of a protein required for directing division to the middle of Escherichia coli. Proc. Natl. Acad. Sci. USA *96*, 4971–4976.
15. Levin, P.A., Shim, J.J., and Grossman, A.D. (1998). Effect of minCD on FtsZ ring position and polar septation in Bacillus subtilis. J. Bacteriol. *180*, 6048–6051.
16. Marston, A.L., Thomaides, H.B., Edwards, D.H., Sharpe, M.E., and Errington, J. (1998). Polar localization of the MinD protein of Bacillus subtilis and its role in selection of the mid-cell division site. Genes Dev. *12*, 3419–3430.
17. Hu, Z., Mukherjee, A., Pichoff, S., and Lutkenhaus, J. (1999). The MinC component of the division site selection system in Escherichia coli interacts with FtsZ to prevent polymerization. Proc. Natl. Acad. Sci. USA *96*, 14819–14824.
18. Scheffers, D.J., de Wit, J.G., den Blaauwen, T., and Driessen, A.J. (2002). GTP hydrolysis of cell division protein FtsZ: Evidence that the active site is formed by the association of monomers. Biochemistry *41*, 521–529.
19. Scheffers, D.J., and Driessen, A.J. (2002). Immediate GTP hydrolysis upon FtsZ polymerization. Mol. Microbiol. *43*, 1517–1521.
20. Justice, S.S., Garcia-Lara, J., and Rothfield, L.I. (2000). Cell division inhibitors SulA and MinC/MinD block septum formation at different steps in the assembly of the Escherichia coli division machinery. Mol. Microbiol. *37*, 410–423.
21. Hu, Z., and Lutkenhaus, J. (2000). Analysis of MinC reveals two independent domains involved in interaction with MinD and FtsZ. J. Bacteriol. *182*, 3965–3971.
22. Cordell, S.C., Anderson, R.E., and Lowe, J. (2001). Crystal structure of the bacterial cell division inhibitor MinC. EMBO J. *20*, 2454–2461.
23. Shiomi, D., and Margolin, W. (2007). The C-terminal domain of MinC inhibits assembly of the Z ring in Escherichia coli. J. Bacteriol. *189*, 236–243.
24. Hu, Z., Saez, C., and Lutkenhaus, J. (2003). Recruitment of MinC, an inhibitor of Z-ring formation, to the membrane in Escherichia coli: Role of MinD and MinE. J. Bacteriol. *185*, 196–203.
25. Johnson, J.E., Lackner, L.L., and de Boer, P.A. (2002). Targeting of (D)MinC/MinD and (D)MinC/DicB complexes to septal rings in Escherichia coli suggests a multistep mechanism for MinC-mediated destruction of nascent FtsZ rings. J. Bacteriol. *184*, 2951–2962.
26. Johnson, J.E., Lackner, L.L., Hale, C.A., and de Boer, P.A. (2004). ZipA is required for targeting of DMinC/DicB, but not DMinC/MinD, complexes to septal ring assemblies in Escherichia coli. J. Bacteriol. *186*, 2418–2429.
27. Lackner, L.L., Raskin, D.M., and de Boer, P.A. (2003). ATP-dependent interactions between Escherichia coli Min proteins and the phospholipid membrane in vitro. J. Bacteriol. *185*, 735–749.
28. Zhou, H., and Lutkenhaus, J. (2003). Membrane binding by MinD involves insertion of hydrophobic residues within the C-terminal amphipathic helix into the bilayer. J. Bacteriol. *185*, 4326–4335.
29. Zhou, H., and Lutkenhaus, J. (2005). MinC mutants deficient in MinD- and DicB-mediated cell division inhibition due to loss of interaction with MinD, DicB, or a septal component. J. Bacteriol. *187*, 2846–2857.
30. Zhou, H., and Lutkenhaus, J. (2004). The switch I and II regions of MinD are required for binding and activating MinC. J. Bacteriol. *186*, 1546–1555.

31. Hu, Z., Gogol, E.P., and Lutkenhaus, J. (2002). Dynamic assembly of MinD on phospholipid vesicles regulated by ATP and MinE. Proc. Natl. Acad. Sci. USA *99*, 6761–6766.
32. Tanford, C. (1961). Physical Chemistry of Macromolecules, First Edition (New York: John Wiley & Sons).
33. Chen, Y., and Erickson, H.P. (2005). Rapid in vitro assembly dynamics and subunit turnover of FtsZ demonstrated by fluorescence resonance energy transfer. J. Biol. Chem. *280*, 22549–22554.
34. Marrington, R., Small, E., Rodger, A., Dafforn, T.R., and Addinall, S.G. (2004). FtsZ fiber bundling is triggered by a conformational change in bound GTP. J. Biol. Chem. *279*, 48821–48829.
35. Small, E., Marrington, R., Rodger, A., Scott, D.J., Sloan, K., Roper, D., Dafforn, T.R., and Addinall, S.G. (2007). FtsZ polymer-bundling by the Escherichia coli ZapA orthologue, YgfE, involves a conformational change in bound GTP. J. Mol. Biol. *369*, 210–221.
36. Anderson, D.E., Gueiros-Filho, F.J., and Erickson, H.P. (2004). Assembly dynamics of FtsZ rings in Bacillus subtilis and Escherichia coli and effects of FtsZ-regulating proteins. J. Bacteriol. *186*, 5775–5781.